4.82. IR (Nujol): ν_{Re-H} 2041, 1953, 1905 cm^{-1}. ^{1}H NMR (298 K): δ 7.1-7.5 (c, 35 H, Ph), 4.32 (s, 4 H, Cp), 4.26 (s, 4 H, Cp), -5.11 (t, $^2J_{PH}$ = 16.2 Hz, 6 H, Re-H). ^{1}H NMR (213 K): δ 7.1-7.6 (c, 35 H, Ph), 4.27 (s, 4 H, Cp), 4.16 (br s, 4 H, Cp), -3.33 (t, $^2J_{PH}$ = 31.2 Hz, 2 H, Re-H), -6.25 (d, $^2J_{PH}$ = 15.4 Hz, 4 H, Re-H). ^{1}H NMR (CD_2Cl_2/$CFCl_3$ 3:2 (v/v), 173 K): δ 6.1-8.0 (c, 35 H, Ph), 4.72 (br s, 2 H, Cp), 4.29 (br s, 2 H, Cp), 4.20 (br s, 2 H, Cp), 3.58 (br s, 2 H, Cp), -3.38 (br t, $^2J_{PH}$ = 31 Hz, 2 H, Re-H), -6.20 (br s, 2 H, Re-H), -6.50 (br s, 2 H, Re-H). Selectively hydride-coupled ^{31}P NMR (298 K): δ 17.7 (heptet, $^2J_{HP}$ = 15.7 Hz). ^{13}C{^{1}H} NMR (298 K): δ 149.4 (s, C_1 of $SiPh_3$), 139.8 (c, C_1 of PPh_2), 136.4 (s, C_2 of $SiPh_3$), 134.1 (t, $^2J_{PC}$ = 11.1 Hz, C_2 of PPh_2), 130.0 (s, C_4 of PPh_2), 127.9 (t, $^3J_{PC}$ = 10.2 Hz, C_3 of PPh_2), 127.3 (s, C_4 of $SiPh_3$), 127.0 (s, C_3 of $SiPh_3$), 78.5 (c, C_1 of Cp), 75.7 (t, $^2J_{PC}$ = 9.3 Hz, C_2 of Cp), 73.2 (t, $^3J_{PC}$ = 5.6 Hz, C_3 of Cp).

$ReH_6(SiPh_3)$(dppb) and $ReH_6(SiPh_3)$\{(+)-diop\} were similarly prepared. Their analytical and spectroscopic data are included in the supplementary material.

Acknowledgment. We thank the National Science Foundation for support, Dr. Peter Demou for assistance, and Dr. Judith A. K. Howard for neutron diffraction data of ReH_7(dppe).

Supplementary Material Available: Analytical and spectroscopic data for *cis*-$ReOCl_3L_2$ complexes, ReH_7L_2 complexes **4-7**, $ReH_6(SiPh_3)$(dppb), and $ReH_6(SiPh_3)$\{(+)-diop\} (5 pages). Ordering information is given on any current masthead page.

Flexibility of the Zeolite RHO Framework. In Situ X-ray and Neutron Powder Structural Characterization of Divalent Cation-Exchanged Zeolite RHO

D. R. Corbin,*,† L. Abrams,† G. A. Jones,† M. M. Eddy,‡ W. T. A. Harrison,‡ G. D. Stucky,‡ and D. E. Cox§

Contribution from the Central Research and Development Department,‖ E. I. du Pont de Nemours and Company, Inc., Experimental Station, P.O. Box 80262, Wilmington, Delaware 19880-0262, Department of Chemistry, University of California at Santa Barbara, Santa Barbara, California 93106, and Physics Department, Brookhaven National Laboratory, Long Island, Upton, New York 11973. *Received May 1, 1989*

Abstract: Zeolite RHO has an unusual three-dimensional monolayer surface with a topology that gives equal access to either side of the surface. In the absence of supporting structural subunits, e.g., smaller cages or channels, RHO exhibits atypical framework flexibility with large displacive rearrangements. These have been investigated by in situ X-ray powder diffraction studies of zeolite RHO exchanged with various divalent cations. The unit cell variation (e.g., Ca,H-RHO (400 °C), a = 13.970 (5) Å; Sr-RHO (250 °C), a = 14.045 (1) Å; Ba-RHO (200 °C), a = 14.184 (2) Å; Cd-RHO (350 °C), a = 14.488 (3) Å; Na,Cs-RHO (25 °C), a = 15.031 (1) Å) is a particularly sensitive function of cation and temperature. Rietveld analysis of neutron diffraction data was used to refine the structures of two samples, Ca,ND_4-RHO and Ca,D-RHO. Ca,D-RHO shows the largest reported deviation from $Im\bar{3}m$ symmetry (a = 13.9645 (7) Å) for a RHO structure. The calcium atom is located in the center of the double 8-ring, distorting the framework to generate a tetrahedral environment. The in situ X-ray studies of zeolite RHO with both monvalent and divalent cations together with the Rietveld results for the extreme end member of this structural field confirm the largest displacive distortion observed for a molecular sieve framework with a unit cell volume increase of 25% when the calcium ions of Ca,H-RHO are replaced with hydrogen ions to give H-RHO.

Zeolites are crystalline aluminosilicate materials with open framework structures of molecular dimensions. The term "open framework" indicates the presence of intracrystalline voids—that is, cages and channels or pore openings. It is the shape and size of these pore openings that give a zeolite its molecular sieving ability and hence shape and size selectivity when used as a catalyst, support, or absorbent. For many years, zeolite frameworks have been known to exhibit small distortions.[1] Recent studies have shown distortions resulting in a change of symmetry on sorption of different solvents[2a] or as a function of temperature.[2b] The observed distortions and their effects on the pore openings are insignificant when compared to the flexiblity and distortions observed in the framework of zeolite RHO.[3] The flexibility in zeolite RHO offers an oppotunity to introduce a high degree of catalytic selectivity by controlled cation siting at reaction temperatures. Our studies of the selective synthesis of dimethylamine from methanol and ammonia over zeolite RHO showed it to exhibit a unique selectivity and activity compared to other small-pore zeolites.[4] This observation led us to further investigate the flexibility of this zeolite framework.

The framework of RHO (Figure 1) is composed of a body-centered cubic arrangement of truncated cubo-octahedra or α-cages linked via double 8-rings. X-ray powder structural studies

† E. I. du Pont de Nemours and Company, Inc.
‡ University of California at Santa Barbara.
§ Brookhaven National Laboratory.
‖ Contribution No. 4930.

(1) Smith, J. V. *J. Chem. Soc.* **1964**, 3759.

(2) (a) Fyfe, C. A.; Kennedy, G. J.; De Schutter, C. T.; Kokotailo, G. T. *J. Chem. Soc.* **1984**, 541-542. Fyfe, C. A.; Stobl, H.; Kokotailo, G. T.; Kennedy, G. J.; Barlow, G. F. *J. Am. Chem. Soc.* **1988**, *110*, 3373-3380. Schlenker, J. L.; Pluth, J. J.; Smith, J. V. *Mater. Res. Bull.* **1979**, *14*, 751 and references therein. (b) Bennett, J. M.; Blackwell, C. S.; Cox, D. E. In *Intrazeolite Chemistry*; Stucky, G. D., Dwyer, F. G., Eds.; American Chemical Society: Washington, DC, 1983; Adv. Chem. Ser. 218 pp 143-158. Bennett, J. M.; Blackwell, C. S.; Cox, D. E. *J. Phys. Chem.* **1983**, *87*, 3783-3790. Hay, D. G.; Jaeger, H.; West, G. W. *J. Phys. Chem.* **1985**, *89*, 1070-1072.

(3) Natrolite, with a small kinetic channel diameter of 2.6 Å that will admit molecules smaller than ammonia, also has large framework distortions. (See: Baur, W. H.; Fischer, R. X.; Shannon, R. D. In *Innovation in Zeolite Materials Science*; Grobet, P. J., et al., Eds; Elsevier Science: Amsterdam, 1988; pp 281-292.)

(4) Keane, M.; Sonnichsen, G. C.; Abrams, L.; Corbin, D. R.; Gier, T. E.; Shannon, R. D. *Appl. Catal.* **1987**, *32*, 361. Shannon, R. D.; Keane, M., Jr.; Abrams, L.; Staley, R. H.; Gier, T. E.; Corbin, D. R.; Sonnichsen, G. C. *J. Catal.* **1988**, *114*, 8-16. Shannon, R. D.; Keane, M., Jr.; Abrams, L.; Staley, R. H.; Gier, T. E.; Corbin, D. R.; Sonnichsen, G. C. *J. Catal.* **1988**, *113*, 367-382. Bergna, H. E.; Corbin, D. R.; Sonnichsen, G. C. U.S. Patent 4683334, 1987. Bergna, H. E.; Corbin, D. R.; Sonnichsen, G. C. U.S. Patent 4752596, 1988. Gier, T. E.; Shannon, R. D.; Sonnichsen, G. C.; Corbin, D. R.; Keane, M., Jr. U.S. Patent 4806689, 1989. Abrams, L.; Corbin, D. R.; Shannon, R. D. U.S. Patent 4814503, 1989.

0002-7863/90/1512-4821$02.50/0

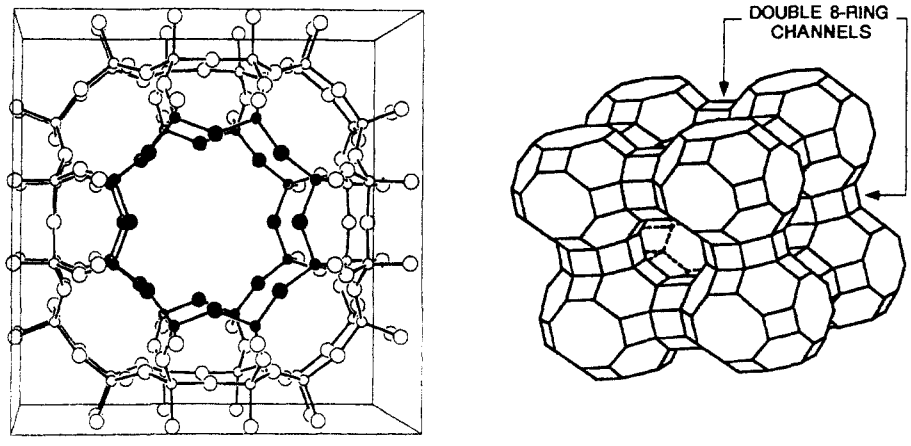

a b

Figure 1. (a) The framework structure of dehydrated zeolite H-RHO[33] with full $Im\bar{3}m$ symmetry showing the cage structure. The six-ring windows are each directly connected to a second cage with similar eight-ring openings to give the double eight-ring openings in part b. (b) Interpenetrating eight-ring channel and cage structure of dehydrated zeolite H-RHO[33] with full $Im\bar{3}m$ symmetry.

by McCusker and Baerlocher[5] have shown that the cation-exchanged RHO undergoes distortion and loss of symmetry upon dehydration. The hydrated, partially sodium-exchanged Na,Cs-RHO exhibits centrosymmetric $Im\bar{3}m$ symmetry; however, upon dehydration, a tetrahedral deformation of the α-cages occurs to give the noncentrosymmetric space group, $I\bar{4}3m$. This change in symmetry is directly related to a 2.3% decrease in the lattice parameter from 15.031 (1) to 14.678 (1) Å. These overall features were first elucidated by Robson and co-workers.[6] Their refinements of X-ray powder film data indicated the structure described above, which had been proposed as a hypothetical zeolite structure earlier by Moore and Smith[7] and later by Meier and Kokotailo.[8] Despite good refinements in the space group $Im\bar{3}m$, the final residuals remained high, so lowering of the symmetry was attempted. The most significant improvement resulted from use of the subgroup $I\bar{4}3m$. However, the resulting bond lengths were chemically unreasonable.

McCusker[9] studied the deformation of the RHO framework occurring upon deammoniation. The ammonium form, ideally $(NH_4)_{12}Al_{12}Si_{36}O_{96}$, has a structure with a = 14.821 (1) Å, while in the hydrogen form, the framework shows little if any deviation from the ideal $Im\bar{3}m$ symmetry even at 500 °C. Parise and co-workers[10] found, from neutron powder refinements on the hydrated (D_2O-RHO) form, that the cell refined in the centrosymmetric space group with a = 15.027 (2) Å. The distortion of the dehydrated (D-RHO) form clearly showed a temperature dependence.[11] At 11 K, the cell refined in the noncentrosymmetric space group with a cell edge of about 14.601 (1) Å. With increasing temperature the degree of the distortion of the cell decreased and finally disappeared above 800 K.

Parise et al.[12] defined a parameter, Δ, to describe the distortion or ellipticity of the double 8-ring whose major axes are orthogonal to each other. The effective cross-section of these rings and the size and shape of the openings connecting α-cages is related to Δ. For other zeolites, control over ring aperture dimensions is achieved typically by using different sized cations as in zeolites 3A, 4A, and 5A. The cations K^+, Na^+, and Ca^{2+} in the A framework eclipse the ring opening to varying degrees depending on their size and population. However, for zeolite RHO, it appeared to us that the framework itself could be used to modify the cage openings without actually blocking those openings.[13,14]

Recently, we reported our initial observations describing the nature of framework distortions caused by cations in the absence of adsorbed molecular species.[15,16] In the case of other cation-substituted zeolites, charge compensation may produce lattice strain sufficient to promote decomposition of that zeolite under mild conditions.[17] By virtue of its flexibility, the RHO framework is able to distort and relieve the strain imposed by the charge-compensating ions. We have therefore embarked on a systematic study of the effect of the charge-compensating monovalent and divalent cations on the framework distortion of zeolite RHO.

Our earlier results suggested that the degree of distortion of the framework is related to the charge density of the cation. Partial reammoniation of H-RHO ($a \sim$ 15.1 Å) yields a cell of 14.4254 (5) Å. Even greater distortion of the cell is dependent on the specific monovalent ion exchange; for example, Li,Cs-RHO and Ag-RHO produce cell edges of 14.4925 (5) and 14.2251 (6) Å, respectively.[15,16] In this paper, we extend our studies to describe the effect of divalent ions and our results of in situ X-ray powder diffraction studies and structure refinement from neutron diffraction data of two divalent exchanged samples, Ca,ND_4-RHO and Ca,D-RHO.[18] An overview is presented of the relation between the topological distortion and specific changes in framework atom bond lengths and angles. This is over a distortion range that has not been previously accessible for a single zeolite phase that has useful catalytic properties.

Experimental Section

Ca,Cs-RHO. Na,Cs-RHO was prepared by a modification of the method described by Robson.[19] Batches were prepared by adding 720

(5) McCusker, L. B.; Baerlocher, C. In *Proceedings of the Sixth International Zeolite Conference*; Olson, D., Bisio, A., Eds.; Butterworths: Guildford, Surry, UK, 1984; pp 812–822.
(6) Robson, H. E.; Shoemaker, D. P.; Ogilvie, R. A.; Manor, P. C. *Adv. Chem. Ser.* **1973**, *121*, 106.
(7) Moore, P. B.; Smith, J. V. *Mineral. Mag.* **1964**, *33*, 1008.
(8) Meier, W. M.; Kokotailo, G. T. *Z. Kristallogr.* **1965**, *121*, 211.
(9) McCusker, L. B. *Zeolites* **1984**, *4*, 51–55.
(10) Parise, J. B.; Gier, T. E.; Corbin, D. R.; Cox, D. E. *J. Phys. Chem.* **1984**, *88*, 1635–1640.
(11) Parise, J. B.; Abrams, L.; Gier, T. E.; Corbin, D. R.; Jorgensen, J. D.; Prince, E. *J. Phys. Chem.* **1984**, *88*, 2303–2307.
(12) Parise, J. B.; Prince, E. *Mater. Res. Bull.* **1983**, *18*, 841–852.
(13) Ca-exchanged RHO has been shown to exhibit enhanced selectivity for methylamines synthesis over H-RHO. Gier, T. E.; Shannon, R. D.; Sonnichsen, G. C.; Corbin, D. R.; Keane, M., Jr. U.S. Patent 4806689, 1989.
(14) Neutron powder structural characterization of Li-RHO (a = 14.3390 (5) Å) exhibits significant framework distortion (as indicated by the relatively small cell edge). The lithium ions site solely in the 6-membered rings leaving the 8-ring windows open (ref 16b).
(15) Corbin, D. R.; Stucky, G. D.; Eddy, M. M.; Prince, E. E.; Abrams, L.; Jones, G. A. *Abstracts of Papers*; 193rd National Meeting of the American Chemical Society, Denver, Colorado, April 1987; American Chemical Society: Washington, D.C., 1987; INOR 300.
(16) (a) Corbin, D. R.; Eddy, M. M.; Stucky, G. D.; Parise, J. B.; Vega, A. J.; Jones, G. A.; Abrams, L.; Cox, D. E. Manuscript in preparation. (b) Stucky, G. D.; Eddy, M. M.; Corbin, D. R.; Abrams, L.; Jones, G. A.; Prince, E. Presented in part at the American Crystallographic Association Meeting, McMaster University, Ontario, Canada, June 1986.
(17) Lutz, W.; Fahlke, B.; Lohse, U.; Buelow, M.; Richter-Mendau, J. *J. Cryst. Res. Technol.* **1983**, *18*(*4*), 513–518.
(18) Preliminary results of this study have been reported. (See: Corbin, D. R.; Abrams, L.; Jones, G. A.; Eddy, M. M.; Stucky, G. D.; Cox, D. E. *J. Chem. Soc., Chem. Commun.* **1989**, 42–43.)
(19) Robson, H. E. U.S. Patent 3720750 (1973).

mL of colloidal silica (Ludox (DuPont) LS-30) to a mixture containing 200 mL of 4 M Na_2AlO_2OH, 56 mL of 50% CsOH, and 32 g of NaOH in polytetrafluoroethylene (Teflon (Corning)) bottles and allowing the solution to stand at room temperature for 6 days. The resulting mixtures were heated at 100 °C for 6 days and then filtered and thoroughly washed with distilled water. The dried powder was shown by X-ray powder diffraction to be highly crystalline zeolite RHO. Chemical analysis gave a unit cell composition of $Na_{7.1}Cs_{3.8}Al_{11.5}Si_{36.5}O_{96}$. Ten grams of this sample were ion exchanged by contacting the zeolite with 1 L of a 1 M solution of $Ca(NO_3)_2$ acidified with 9.6 mL of 0.1 N HNO_3 for 7 days at room temperature. The resulting Ca,Cs-RHO zeolite was filtered and washed thoroughly with distilled water. Chemical analysis gave a unit cell composition of $Ca_{3.4}Cs_{3.8}Na_{0.77}Al_{11.7}Si_{36.3}O_{96}$.

Ca,NH_4-RHO. Na,Cs-RHO was first prepared and then exchanged six times (1 h each) in aqueous 10% NH_4NO_3 (10 mL/g) at 90 °C to give NH_4-RHO. The NH_4-RHO was exchanged twice (24 h each) in aqueous 0.4 M $Ca(NO_3)_2$ (10 mL/g) at 25 °C. Then the sample was exchanged three additional times (24 h each) in aqueous 0.4 M $Ca(NO_3)_2$ (10 mL/g) at 90 °C to give Ca,NH_4-RHO. Chemical analysis gave a unit cell composition of $Ca_{4.0}(NH_4)_{3.3}Na_{0.13}Cs_{0.10}Al_{11.5}Si_{36.5}O_{96}$ with NH_4 assumed from charge balance.

Ca-RHO. The NH_4-RHO as prepared above was exchanged six times (1 h each) in aqueous 10% $NaNO_3$ (10 mL/g) at 90 °C to give Na-RHO. The Na-RHO was exchanged six times (1 h each) in aqueous 10% $Ca(NO_3)_2$ (10 mL/g) at 90 °C to give Ca-RHO. Chemical analysis gave a unit cell composition of $Ca_{5.8}Na_{0.70}Cs_{0.16}A_{11.4}Si_{36.6}O_{96}$.

Sr-RHO. Na-RHO, as prepared above, was exchanged six times (1 h each) in aqueous 10% strontium acetate (10 mL/g) at 90 °C. Chemical analysis gave a unit cell composition of $Sr_{5.2}Na_{0.10}Cs_{0.20}Al_{11.1}Si_{36.9}O_{96}$.

Ba-RHO. Na-RHO, as prepared above, was exchanged six times (1 h each) in aqueous 10% $Ba(NO_3)_2$ (10 mL/g) at 90 °C. Chemical analysis gave a unit cell composition of $Ba_{5.0}Na_{0.10}Cs_{0.23}Al_{11.0}Si_{37.0}O_{96}$.

Cd-RHO. Na-RHO, as prepared above, was exchanged six times (1 h each) in aqueous 10% $Cd(NO_3)_2$ (10 mL/g) at 90 °C. Chemical analysis gave a unit cell composition of $Cd_{4.8}Na_{0.06}Cs_{0.22}Al_{11.0}Si_{37.0}O_{96}$.

In situ X-ray powder diffraction studies of thermally and chemically induced transformations were monitored with a totally automated diffractometer–microreactor system.[20] The equipment was designed for in situ structural studies of gas/liquid/solid and solid/solid interactions in the interval of 0 to 1000 °C. The θ–θ vertical mode goniometer was automated for angular slew and step control, with on-line data collection and conversion for device display, and data transmission through network protocol. Reactor chamber temperature and precursor partial pressure were tailored to multiple-segment scans through an assemblage of microprocessors connected to six mass flow controllers. Phase transitions were surveyed as non-kinetic events through sequential inert gas sweep to 200 mL/min or sample chamber evacuation to 1 mTorr, either at controlled thermal ramp (°C/min/deg 2θ) or isothermal set-point to 1000 °C. For Ca,Cs- and Ca,NH_4-RHO, the samples were dehydrated at 80 °C for 16 h, followed by 2-h hold and 2-h X-ray scan sequences in increments of 50 deg between 100 and 500 °C. The cooling cycle was executed in 100-deg intervals to room temperature, each 2 h in duration for hold and scan. Ca-RHO was run in 2-min ramp and 2-h hold and scan sequences in increments of 100 to 500 deg and down, to room temperature.

Individual ASCII data files of 8000 steps (fixed time) per segment were ordered in 1 to 32 segments per setup file; multiple setups were utilized in each data collection run, that is, desorption under vacuum to the limit of temperature, sorption under controlled partial pressures of helium or ammonia or water to T_{max}, and subsequent desorption in time-dependent ramp-and-hold thermal cycles.

Cell parameters were refined with use of a modified least-squares program after correcting sample peak locations through silicon internal standard thermal expansion reference positions. Generally, the range of refinement in 2θ was limited to 15 to 60°, because of unpredictable systematic errors below the first standard position. Full set refinement acceptance was based on the absence of systematic errors of magnitude exceeding two goniometer steps between approximately 15 and 60° 2θ, and rejection of any reflections whose calculated and observed (refined) difference exceeded two goniometer steps of 0.025 deg/step. Thus, unit cell dimensions are reported with errors at two standard deviations and are without discernible systematic errors under the conditions of the experiment. In instances where two phases were evident at or near the transition temperature, only a single set of standard lines was observed as evidence of sample flatness being maintained over the course of the transition and, ultimately, the experiment.

Point-to-point temperature differences across the length of the 1 in^2 sample preparation did not exceed reported uncertainties of types R, J, or K thermocouples at 500 °C (approximately 3 °C) as monitored by three thermocouples positioned along the sample diagonal.

Deuterated forms (Ca,ND_4-RHO and Ca,D-RHO) were prepared for neutron powder diffraction study as follows.

Ca,ND_4-RHO. A sample of Ca,NH_4-RHO was loaded into a vacuum-tight cell which was attached to a manifold and evacuated while being heated to 250 °C. The sample was kept under vacuum at that temperature for approximately 112 h at which time the sample was subjected to 3 D_2O exposures at 6 Torr and pumped out to approximately 50 mTorr between exposures. After the final exposure, the sample was evacuated at 250 °C for 32 h and then sealed off.

Ca,D-RHO. A sample of Ca,NH_4-RHO was loaded into a vacuum-tight cell which was attached to a manifold and evacuated while being heated to 400 °C. The sample was kept under vacuum at that temperature for approximately 112 h and then cooled to 250 °C. At 250 °C, the sample was subjected to 3 D_2O exposures at 6 Torr and pumped out to approximately 50 mTorr between exposures. After the final exposure, the sample was evacuated at 250 °C for 16 h after which it was again brought to 400 °C under vacuum for an additional 16 h and then sealed off.

Room temperature neutron powder diffraction data were collected on the samples on diffractometer H4S at the High-Flux Beam Reactor, Brookhaven National Laboratory. Structural refinements were carried out with the program GSAS,[21] and in all cases framework atom, bond distance, and angle restraints[22] were used throughout the refinement.

TGA/MS was used to monitor water and ammonia desorption for the ammonium samples on a Du Pont 951 Thermal Gravimetric Analyzer interfaced to a Hewlett Packard 5970 Series Mass Spectrometer.

Results and Discussion

The approach used in this study was to first examine the temperature dependence of the structural changes of the CaCs-, Ca,NH_4-, Ca-, Sr-, Ba-, and Cd-RHO samples by in situ X-ray diffraction methods. Deammoniation and dehydration were monitored by TGA/MS under the same environmental conditions. Those materials, which showed the greatest deviation from $Im\bar{3}m$ symmetry (smallest cell parameters) under similar thermal ramp-and-hold collection strategies, were subsequently used for detailed structural analysis on deuterated samples upon data collection at B.N.L.

Examples of the powder diffraction patterns resulting from the in situ X-ray diffraction studies of the vacuum dehydration are given in Figures 2 (Ca,NH_4-RHO) and 3 (Cd-RHO). (Sequences of X-ray diffraction patterns for Ca,Cs-RHO, Ca-RHO, Sr-RHO, and Ba-RHO are available as supplementary material.) The variations in the different unit cell dimensions (Ca,Cs-, Ca,NH_4-, Ca-, Sr-, Ba-, and Cd-RHO) are illustrated in Figure 4A–F. (The refined unit cell dimensions are also available as supplementary material.) The Ca-exchanged samples of zeolite RHO are unique in a number of respects with the smallest known unit cells for zeolite RHO, and for this reason they are discussed below in detail.

Upon heating under vacuum to 50 °C, the Ca,Cs-RHO sample loses water and the cell contracts from about 15.0 to 14.6 Å (see Figure 4A). Unlike most of the previously studied systems of the ion-exchanged RHO,[15,16] further heating to 500 °C leads to contraction of the cell to about 14.34 Å. Upon cooling to room temperature, the cell expands to about 14.5 Å. This unusual behavior prompted us to examine the effect of calcium (in the absence of cesium) on the framework of zeolite RHO. The unit cell of Ca,NH_4-RHO (see Figures 2 and 4B) contracts from 14.45 to about 14.0 Å, at 250 °C, the smallest cell edge yet observed for zeolite RHO. Upon cooling, the cell expands at 100 °C and then contracts on reaching room temperature. A TGA/MS investigation on the original Ca,NH_4-RHO sample revealed two major events during heating. One centered at approximately 100 °C corresponds primarily to sample dehydration/deammoniation and another centered at 400 °C corresponds to the evolution of

(20) Jones, G. A. Presented in part at the American Crystallographic Association Meeting, Stanford University, Palo Alto, CA, 1985. Jones, G. A. Presented in part at the Thirteenth International Congress of Crystallography, Hamburg, FRG, 1984. Jones, G. A. Presented in part at the FASS Meeting, Philadelphia, PA, 1982.

(21) von Dreele, R. B.; Larsen, A. C. Los Alamos Report LAUR 86-748.

(22) Baerlocher, C. In *Proceedings of the Sixth International Zeolite Conference*; Olson, D., Bisio, A., Eds.; Butterworths: Guildford, Surry, UK, 1984; pp 823–833. Waser, J. *Acta Cryst.* **1963**, *16*, 1091.

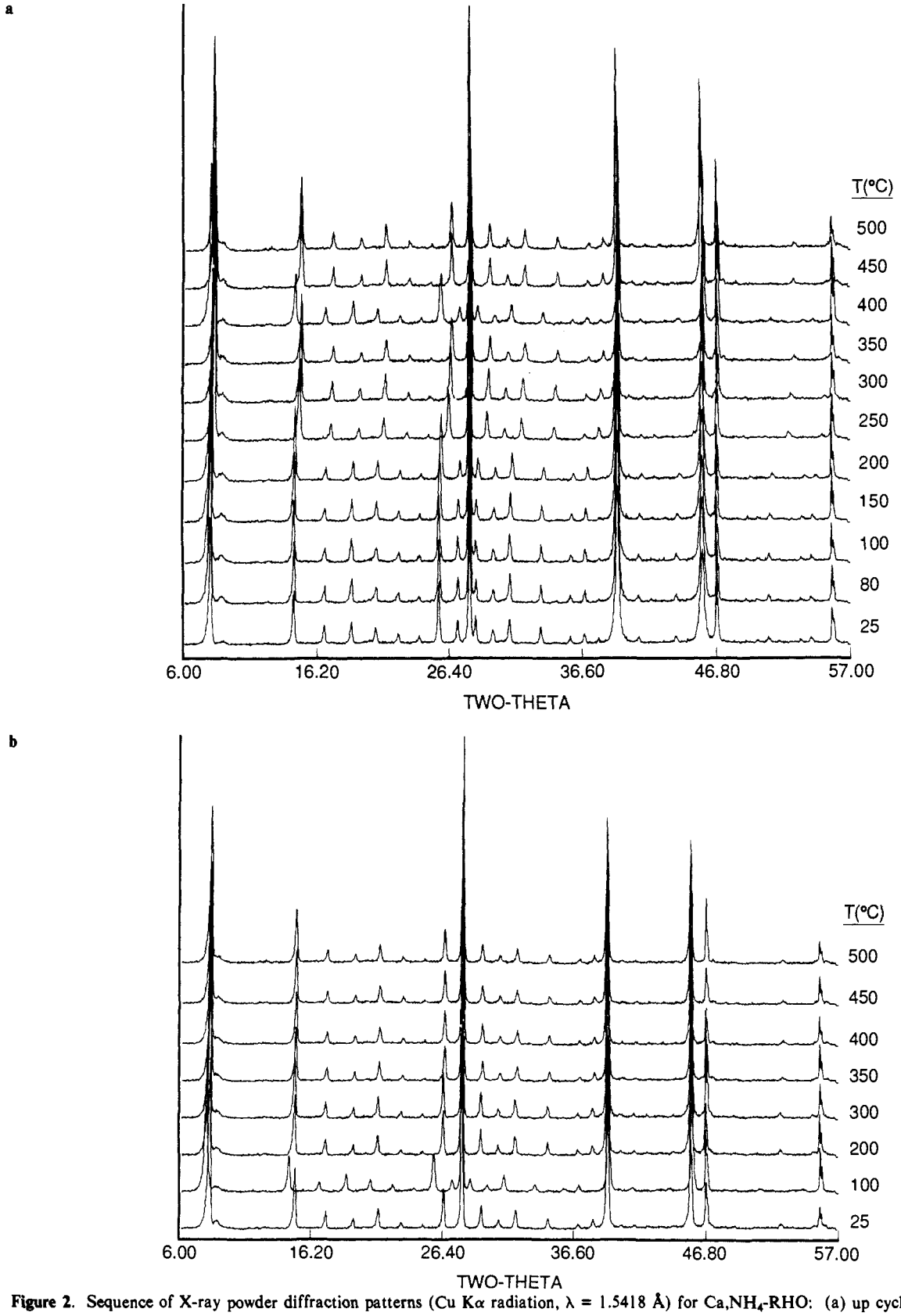

Figure 2. Sequence of X-ray powder diffraction patterns (Cu Kα radiation, λ = 1.5418 Å) for Ca,NH_4-RHO: (a) up cycle and (b) down cycle.

ammonia. This second event may be related to the anomalous cell expansion observed upon heating to 400 °C in the in situ X-ray diffraction experiment. Finally, in situ X-ray diffraction studies of the Ca-RHO sample (see Figure 4C) show water loss above 200 °C resulting in a reduction in unit cell size from 14.4 to 14.0 Å.

The observation of these highly distorted cells provoked the question of the siting of the Ca^{2+} ions and the determination of the structure of Ca,ND_4-RHO from powder neutron diffraction experiments. At room temperature, two phases coexist in this sample as shown in Figure 5A, which shows the final observed, calculated, and difference profiles from a two-phase Rietveld analysis of the data. The phases are defined as Phase 1 (high ND_4/low Ca, a = 14.410 (2) Å, and Phase 2 (low ND_4/high Ca, a = 14.110 (1) Å), and refined atomic parameters and residuals for both phases are given in Table I with selected bond distances

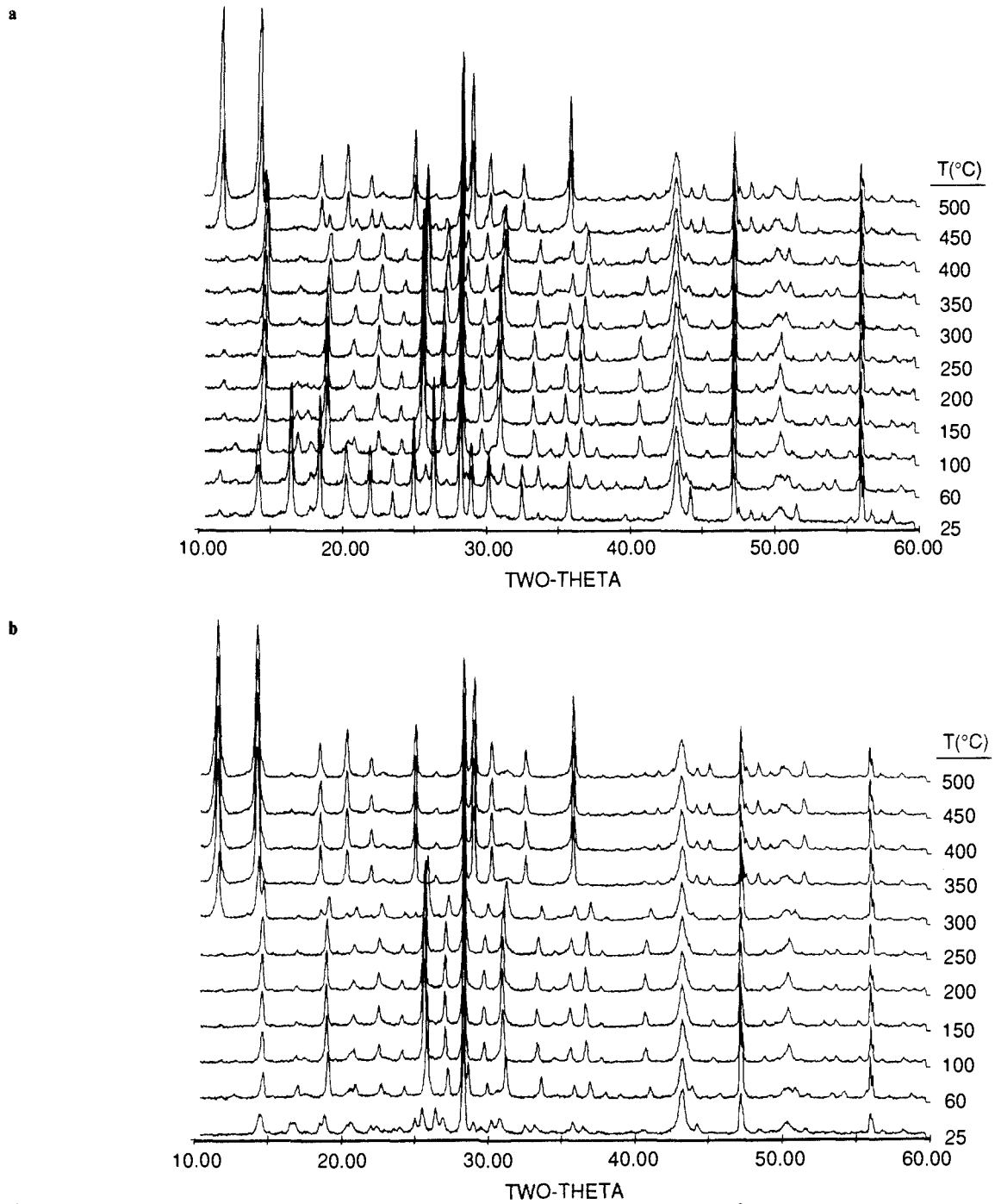

Figure 3. Sequence of X-ray powder diffraction patterns (Cu Kα radiation, λ = 1.5418 Å) for Cd-RHO: (a) up cycle and (b) down cycle.

and angles in Table II. It was not possible to resolve the relative ND_4/Ca occupancies for these phases as the ions are at the same extra-framework cation site located and refined at the center of the double eight-ring. The phase with the smaller unit cell dimension (Phase 2) has the larger calcium content, which distorts the eight-ring ellipse more than the bulky univalent ND_4 cation (Phase 1). It is interesting that the cell edge of Phase 1 is close to that observed at 400 °C on heating the Ca,NH_4-RHO in the in situ X-ray diffraction experiment. Data obtained for the two-phase sample after heating to 400 °C, however, show that this sample is a single-phase Ca,D-RHO, resulting from deammoniation and a redistribution of the Ca^{2+} cations. The results of the refinement are given in Table III with selected bond distances and angles in Table IV. The corresponding observed, calculated, and difference profiles are shown in Figure 5b.

The framework structure of the double 8-ring for Ca,D-RHO is illustrated in Figure 6. Figure 7 shows the framework structural changes from dehydrated H-RHO ($Im\bar{3}m$) to Ca,D-RHO ($I\bar{4}3m$). It should be noted that the double eight-rings are connected between cages as "crossed ellipses" (Figures 6 and 7c). The calcium cations are located at the center of the orthogonal double eight-ring, tetrahedrally coordinated to four framework oxygen atoms (Ca–O = 2.70 (1) Å). This distorts the eight-rings into highly anisotropic ellipses, in which Δ, the difference of the major and minor axes,[12] is significantly greater than anything yet observed (2.49 Å). Framework distortion is driven by the cation siting to determine the lowest energy state of an ion-exchanged zeolite. In calcium-exchanged zeolite A, the calcium ions are sited in a trigonal environment within the 6-rings of the α-cage.[23] In Ca,D-RHO, the calcium ions reside in a very unusual and strained tetrahedral environment. Upon removal of water, the cations must use whatever charge-compensating coordination is available, and in this case the flexibility of the framework provides a tetrahedral

(23) Pluth, J. J.; Smith, J. V. *J. Am. Chem. Soc.* **1983**, *105*, 1192.

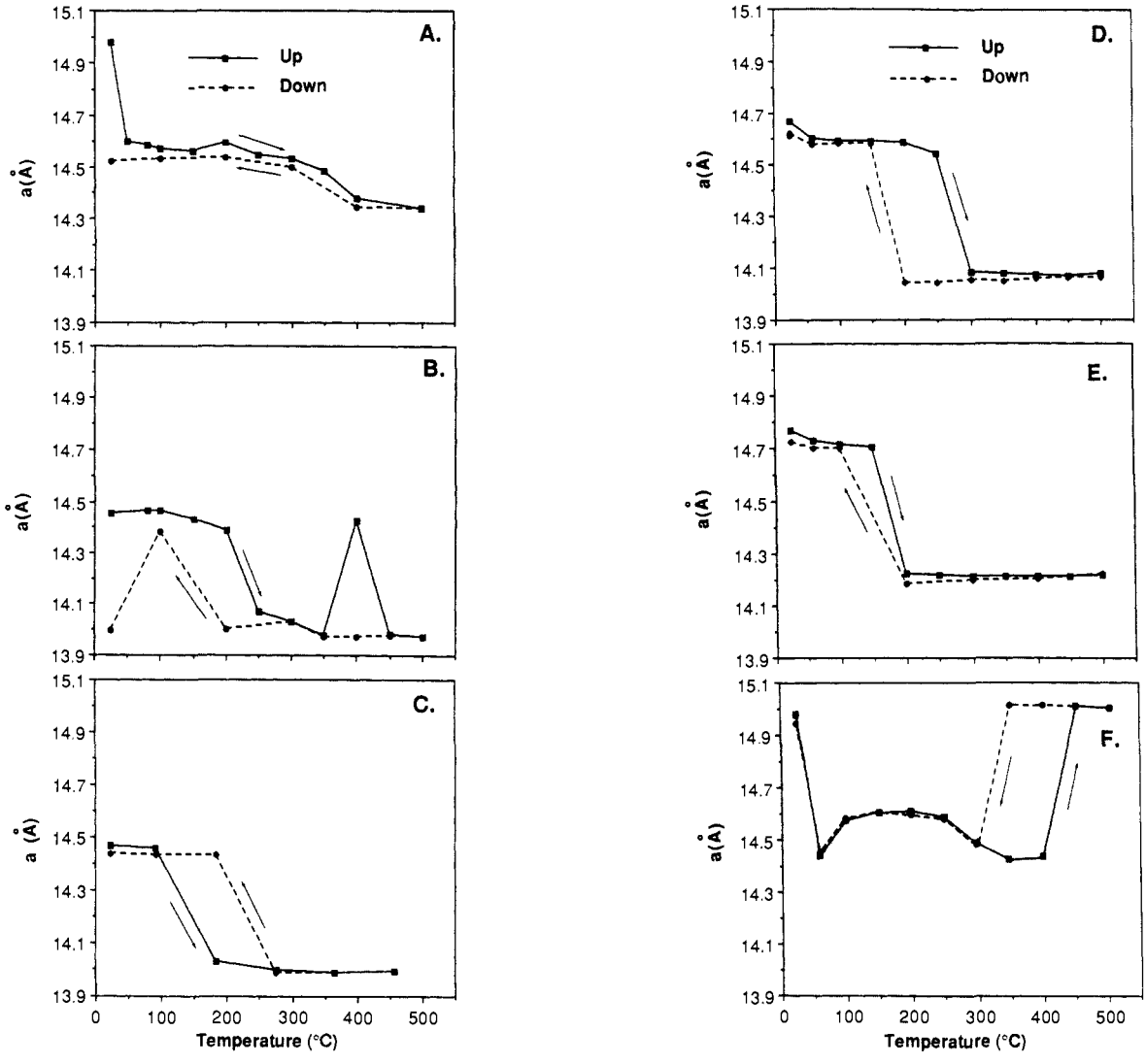

Figure 4. Variation of cell dimension with temperature for (A) Ca,Cs-RHO, (B) Ca,NH_4-RHO, (C) Ca-RHO, (D) Sr-RHO, (E) Ba-RHO, and (F) Cd-RHO.

Table I. Refined Atomic Parameters for Ca,ND_4-RHO Space Group $I\bar{4}3m$ (International Tables No. 217)

atom	x	y	z	B(iso)	pop.
		Phase 1			
T(1)	0.2728 (12)	0.1205 (12)	0.4266 (14)	1.7 (7)	48
O(1)	0.2181 (14)	0.2181 (14)	0.4046 (26)	1.7 (7)	24
O(2)	0.1261 (17)	0.1261 (17)	0.6182 (20)	1.7 (7)	24
O(3)	0.0370 (14)	0.2029 (15)	0.3924 (15)	1.7 (7)	48
N(1)	0.5	0.0	0.0	4.0[c]	4.1 (2)
a = 14.410 (2) Å; R_p[a] = 9.1%; R_{wp}[b] = 11.5%; scale = 19700					
		Phase 2			
T(1)	0.2759 (11)	0.1274 (11)	0.4306 (13)	1.7 (5)	48
O(1)	0.2324 (12)	0.2324 (12)	0.4110 (19)	1.7 (5)	24
O(2)	0.1185 (14)	0.1185 (14)	0.6238 (18)	1.7 (7)	24
O(3)	0.0441 (11)	0.2082 (13)	0.3869 (13)	1.7 (7)	48
Ca(1)	0.5	0.0	0.0	4.0[c]	6
a = 14.110 (1) Å; R_p[a] = 16.1%; R_{wp}[b] = 21.8%; scale = 10919					

[a] $R_p = S_i|y_{oi} - 1/C \cdot y_{ci}|/S_i y_{oi}$. [b] $R_{wp} = [S_i w_i(y_{oi} - 1/C \cdot y_{ci})^2/S_i w_i y_{oi}^2]^{1/2}$. [c] Not refined.

environment rather than the trigonal site associated with the six-ring. The significant distortion of the RHO framework by the calcium ion attests to the strong interaction between the framework and the ion. The lack of degradation of the sample upon calcination to 500 °C is additional evidence of the stability of the RHO framework imparted by its ability to distort. It should also be noted that Li^+ cations in zeolite RHO can be used to control the 8-ring channel opening (Δ), without obstruction of the channel by the cation in contrast to the siting found for Ca^{2+}.[14,16b]

Table II. Selected Bond Lengths (Å) and Angles (deg) for Ca,ND_4-RHO

	Phase 1		
T–O(1)	1.643 (12)	O(1)–T–O(2)	110 (1)
T–O(2)	1.643 (12)	O(1)–T–O(3)	112 (1)
T–O(3)	1.638 (13)	O(1)–T–O(3)	105 (1)
T–O(3)	1.646 (12)	O(2)–T–O(3)	104 (1)
		O(2)–T–O(3)	112 (1)
N(1)–4 × O(3)	3.08 (3)	O(2)–T–O(3)	109 (1)
T–O(1)–T	142 (1)		
T–O(2)–T	145 (1)	Δ[a] = 1.92 Å	
T–O(3)–T	128 (1)		
	Phase 2		
T–O(1)	1.627 (14)	O(1)–T–O(2)	111 (1)
T–O(2)	1.644 (14)	O(1)–T–O(3)	106 (1)
T–O(3)	1.630 (15)	O(1)–T–O(3)	109 (1)
T–O(3)	1.635 (14)	O(2)–T–O(3)	107 (1)
		O(2)–T–O(3)	110 (1)
Ca(1)–4 × O(3)	2.94 (4)	O(2)–T–O(3)	111 (1)
T–O(1)–T	131 (1)		
T–O(2)–T	132 (1)	Δ[a] = 2.31 Å	
T–O(3)–T	140 (1)		

[a] The Δ parameter is defined in the text and in ref 12.

The dependency of the Δ parameter on cell dimensions from 13.9645 to 15.0976 Å is shown in Figure 8 and Table V. The

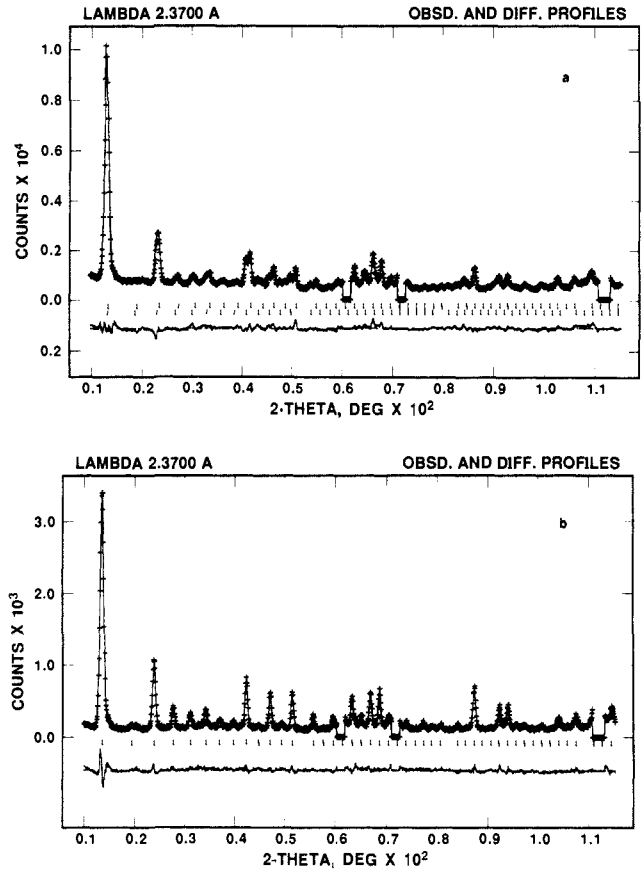

Figure 5. Final calculated (line) and observed (crosses) neutron powder diffraction profiles for (a) Ca,ND_4-RHO and (b) Ca,D-RHO. In each case, the difference pattern (observed minus calculated) is shown below on the same scale as the observed pattern. Tickmarks at the bottom line of the profile indicate peak positions.

Table III. Final Parameters for Ca,D-RHO Space Group $I\bar{4}3m$ (International Tables No. 217)

atom	*x*	*y*	*z*	*B*(iso)	pop.
T(1)	0.2816 (10)	0.1310 (10)	0.4345 (10)	4.0 (7)	48
O(1)	0.2365 (7)	0.2365 (7)	0.4141 (8)	4.3 (6)	24
O(2)	0.1104 (7)	0.1104 (7)	0.6142 (9)	4.7 (7)	24
O(3)	0.0481 (6)	0.2032 (7)	0.3913 (7)	3.3 (5)	48
Ca(1)	0.5	0.0	0.0	6.0[c]	3.4 (1)

a = 13.9645 (7) Å; R_p[a] = 9.6%; R_{wp}[b] = 12.6%

[a] $R_p = S_i|y_{oi} - 1/C \cdot y_{ci}|/S_i y_{oi}$. [b] $R_{wp} = [S_i w_i(y_{oi} - 1/C \cdot y_{ci})^2/S_i w_i y_{oi}^2]^{1/2}$. [c] Not refined.

Table IV. Selected Bond Lengths (Å) and Angles (deg) for Ca,D-RHO

T–O(1)	1.621 (12)	O(1)–T–O(2)	115 (1)
T–O(2)	1.649 (13)	O(1)–T–O(3)	113 (1)
T–O(3)	1.631 (14)	O(1)–T–O(3)	107 (1)
T–O(3)	1.704 (14)	O(2)–T–O(3)	102 (1)
		O(2)–T–O(3)	110 (1)
Ca(1)–4 × O(2)	2.70 (1)	O(2)–T–O(3)	107 (1)
T–O(1)–T	133 (1)		
T–O(2)–T	132 (1)	Δ[a] = 2.49 Å	
T–O(3)–T	130 (1)		

[a] The Δ parameter is defined in the text and in ref 12.

data show an almost linear dependence from a = 14.2 to 14.7 Å with a shift to nonlinearity outside that range. The new data obtained in this study present an unusual opportunity to examine structural trends and framework flexibility in aluminosilicate molecular sieves. The variation of the average T–O (T = (Si, Al)) bond length (⟨T–O⟩) versus cell edge is shown in Figure 9. Linear regression analysis of the data (R^2 = 0.72) in Table V collected at room temperature (excluding hydrated samples) shows

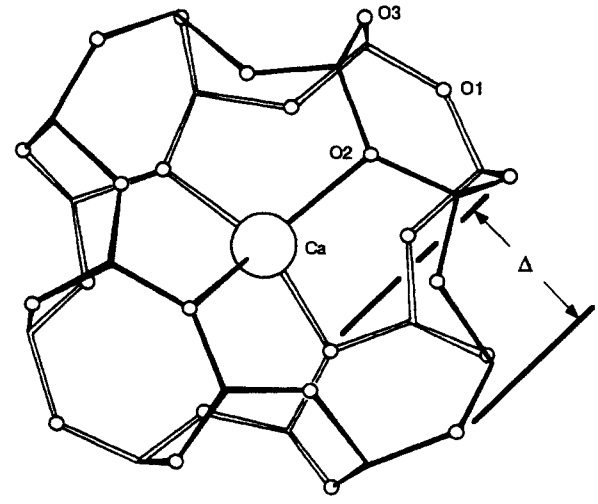

Figure 6. The framework structure of the double 8-ring for Ca,D-RHO.

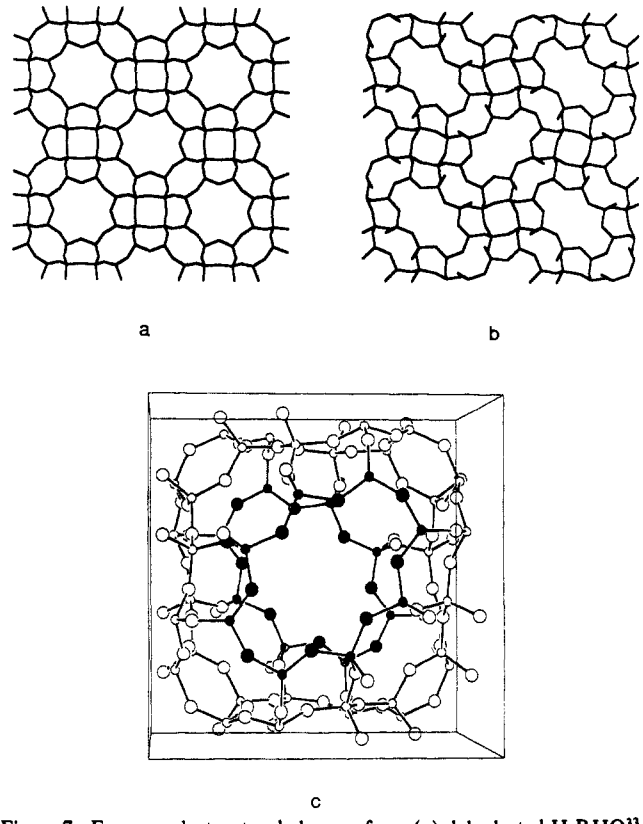

Figure 7. Framework structural changes from (a) dehydrated H-RHO[33] ($Im\bar{3}m$) to (b) Ca,D-RHO ($I\bar{4}3m$). Part c shows the cage structure for Ca,D-RHO.

a systematic increase in ⟨T–O⟩ as the unit cell dimensions decrease. The average T–O–T bond angle (⟨T–O–T⟩) systematically (R^2 = 0.91) decreases with cell edge (Figure 10). The correlation (R^2 = 0.90) of decreasing ⟨T–O–T⟩ bond angle with increasing ⟨T–O⟩ bond length shown in Figure 11 has been described previously for Si–O–Si linkages by Gibbs and co-workers.[24] For a decrease in Si–O–Si bond angle from 147° to 131°, a decrease of 0.03 Å is predicted in the Si–O bond length. This agrees remarkably well with the observed structural variations in zeolite RHO even though some of the linkages are Si–O–Al. The importance of cation-framework coordination in generating T–O framework distortions has been noted previously in single-crystal studies of the mordenite and chabazite families.[25,26] In Figure

(24) Gibbs, G. V.; Meagher, E. P.; Newton, M. D.; Swanson, D. K. *Struct. Bonding Cryst.* **1981**, *1*, 195–225.

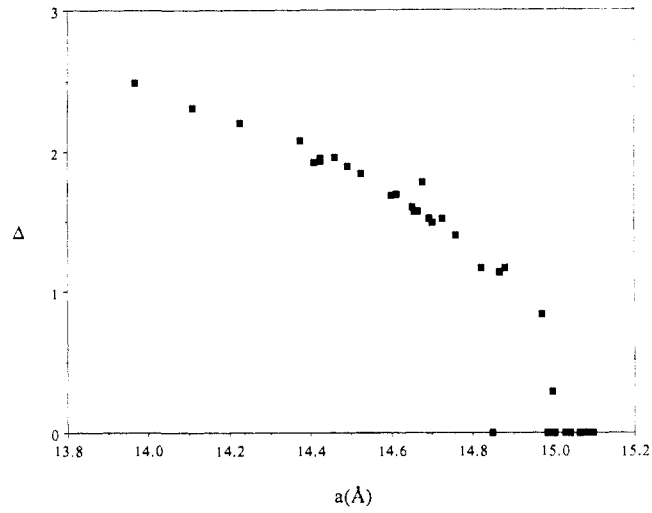

Figure 8. Scatter plot of cell edge (a) versus Δ.

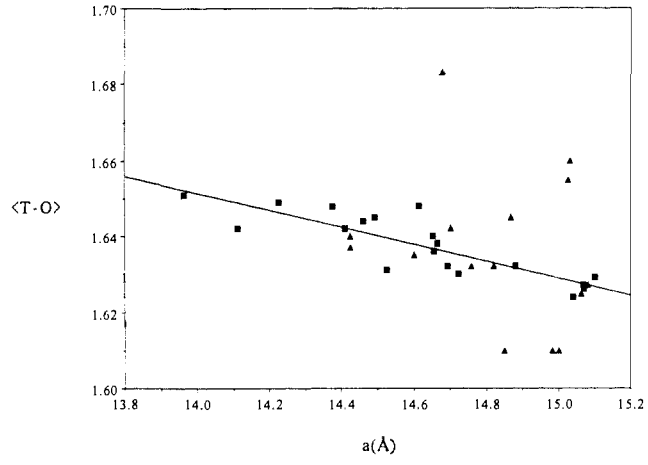

Figure 9. Variation of cell edge (a) versus ⟨T–O⟩ (filled squares, room temperature data (excluding hydrated samples); filled triangles, all data).

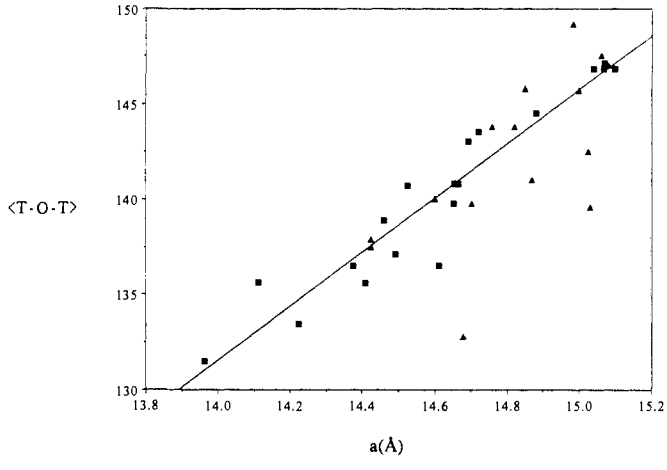

Figure 10. Variation of cell edge (a) versus ⟨T–O–T⟩ (filled squares, room temperature data (excluding hydrated samples); filled triangles, all data).

12, the variation of ⟨T–O⟩ versus f_s,[24] where f_s (using the notation of Gibbs) is equal to $1/(1 - \sec(\langle T\text{–}O\text{–}T\rangle))$, is given. Although f_s neglects the cation coordination and thermal motion,[24,27] good

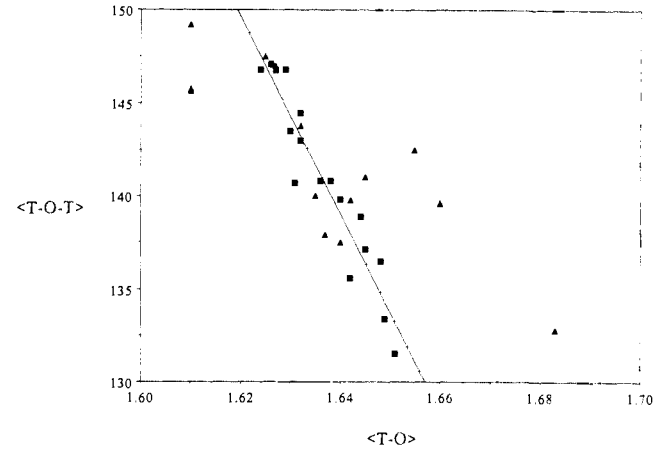

Figure 11. Variation of ⟨T–O⟩ versus ⟨T–O–T⟩ (filled squares, room temperature data (excluding hydrated samples); filled triangles, all data).

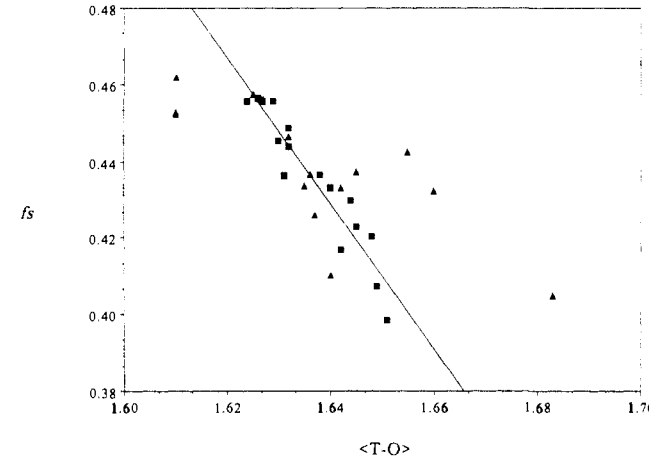

Figure 12. Variation of ⟨T–O⟩ versus f_s (filled squares, room temperature data (excluding hydrated samples); filled triangles, all data).

agreement (R^2 = 0.88) is obtained.

As noted by Gibbs et al.,[24] the potential surface for Si–O–Si bond distortions has a very broad minimum. As a consequence, distance least-squares (DLS) modeling can be easily directed to a variety of non-unique configurations in a structure as flexible as that of zeolite RHO, and in fact it has little predictive value unless particularly well defined constraints are used. These constrants are best obtained from experimental observations such as those available over the wide range of zeolite RHO unit cells. With this limitation in mind, we have used the observed values of ⟨T–O⟩, T–O(1)–T, T–O(2)–T, and T–O(3)–T as determined by regression analysis to define constraints to predict by DLS if even smaller channel windows and cubic cells are accessible. DLS calculations were performed with the Oxford CRYSTALS systems.[28] For progressively smaller values of the unit cell edge, an average T–O bond distance and a single average T–O–T bond angle were determined from the observed trends as plotted in Figures 9 and 10. The structural model was then optimized in space group $I\bar{4}3m$ by using the bond and angle restraints as determined above, as well as the angles defining a regular TO_4 tetrahedron. No second-nearest-neighbor restraints were included in the refinements.

With these particular restraints, the refinements suggest that the limiting factor in unit-cell contraction and framework distortion is the O(2)–O(3) contact between adjacent tetrahedra.[29] For

(25) Smith, J. V. *Mater. Res. Bull.* **1979**, *14*, 849–856. Schlenker, J. L.; Pluth, J. J.; Smith, J. V. *Mater. Res. Bull.* **1979**, *14*, 751–758.
(26) Mortier, W. J. *Mater. Res. Bull.* **1977**, *12*, 103–108. Mortier, W. J.; Pluth, J. J.; Smith, J. V. *Mater. Res. Bull.* **1977**, *12*, 97–102. Mortier, W. J.; Pluth, J. J.; Smith, J. V. *Mater. Res. Bull.* **1977**, *12*, 241–250.
(27) Liebau, F. *Structural Chemistry of Silicates-Structure, Bonding, and Classification*; Springer-Verlag: Germany, 1985; Chapter 3.

(28) (a) Watkin, D. J.; Carruthers, J. R.; Betteridge, P. W. *CRYSTALS User Guide*; Chemical Crystallography Laboratory, Oxford University, 1985. (b) Pawley, G. S. In *Advances in Structural Research by Diffraction Methods*; Hoppe, W., Mason, R., Eds.; Pergammon Press: Oxford, 1972; Vol. 4.
(29) Baur, W. H.; Fischer, R. X.; Shannon, R. D. In *Innovation in Zeolite Materials Science*; Grobet, P. J., et al., Eds; Elsevier Science: Amsterdam, 1988; pp 281–292. Fischer, R. X.; Baur, W. H.; Shannon, R. D.; Parise, J. B.; Faber, J.; Prince, E. *Acta Cryst.* **1989**, *C45*, 983–989.

Table V. Summary of RHO Structural Data

Form	Temperature(K)	a(Å)	Δ(Å)	<T-O>	<T-O-T>	Reference	8-Ring Configuration
CaD	298	13.9645	2.49	1.651	131.5	a	
Sr	473	14.045				15,a	
$CaND_4$(II)	298	14.110	2.31	1.642	135.6	a	Δ = 2.49
Ba	473	14.184				15,a	
Ag	298	14.2251	2.21	1.649	133.4	15,16	
Li	298	14.3390	2.33	1.66		15,16	
$LiND_4$	298	14.372				15,16	
Rb	298	14.375	2.08	1.648	136.5	16	Δ = 2.21
$CaND_4$(I)	298	14.410	1.92	1.642	135.6	a	
$(ND_4)_8$	11	14.4245	1.95	1.640	137.5	11,15,16	
$(ND_4)_8$	11	14.425	1.93	1.637	137.9	30	
Tl	298	14.461	1.96	1.644	138.9	16	
Na	298	14.4848	2.11	1.655	136.3	15,16	
Cd	623	14.488				15,a	
LiCs	298	14.4925	1.89	1.645	137.1	15,16	
$(ND_4)_8$	298	14.5264	1.84	1.631	140.7	29	
D	11	14.601	1.68	1.635	140.0	11	
K	298	14.613	1.69	1.648	136.5	16	
D	13	14.620				30	Δ = 1.92
CsD	298	14.6536	1.60	1.640	139.8	12	
$NaCs(H_2O)$	298	14.6566	1.57	1.636	140.8	29,31	
CsD	298	14.6652	1.57	1.638	140.8	12	
NaCs	298	14.678	1.78	1.683	132.8	5	
dD	294	14.694	1.52	1.632	143.0	10	
CsD	493	14.7014	1.49	1.642	139.8	12	
D	295	14.7237	1.52	1.630	143.5	11	Δ = 1.57
$K(H_2O)$	298	14.7412				15	
D	423	14.7580	1.40	1.632	143.8	11	
$(NH_4)_{12}$	373	14.821	1.17	1.632	143.8	9	
D	13	14.850	0	1.610	145.8	30	
D	573	14.8680	1.14	1.645	141.0	11	
D	298	14.8803	1.17	1.632	144.5	32	
CD_3OD	11	14.969	0.84			11	
H	773	14.982	0	1.610	149.2	9	
Ca		14.995	0.29			11	
H	293	15.00	0	1.610	145.7	6	
D_2O	423	15.027	0	1.655	142.5	10	
$NaCs(H_2O)$	298	15.031	0	1.660	139.6	5	
D	298	15.0387	0	1.624	146.8	32	
D	623	15.0620	0	1.625	147.5	32	Δ = 0
D	298	15.0686	0	1.627	146.8	33	
D	298	15.0696	0	1.626	147.1	33	
D	623	15.0799	0	1.627	147.0	33	
D	298	15.0976	0	1.629	146.8	33	

a. This work.

a = 13.8 Å, this distance is 2.59 Å, reducing to 2.54 Å at a = 13.4 Å. None of the other distances and angles appear over-strained. Of course, this contact could be relieved by a distortion that we have not modeled by the simple DLS refinement.

(30) Fischer, R. X.; Baur, W. H.; Shannon, R. D.; Staley, R. H.; Vega, A. J.; Abrams, L.; Prince, E. *J. Phys. Chem.* **1986**, *90*, 4414.

(31) Baur, W. H.; Bieniok, A.; Shannon, R. D.; Prince, E. *Z. Kristallogr.* **1989**, *187*, 253–266.

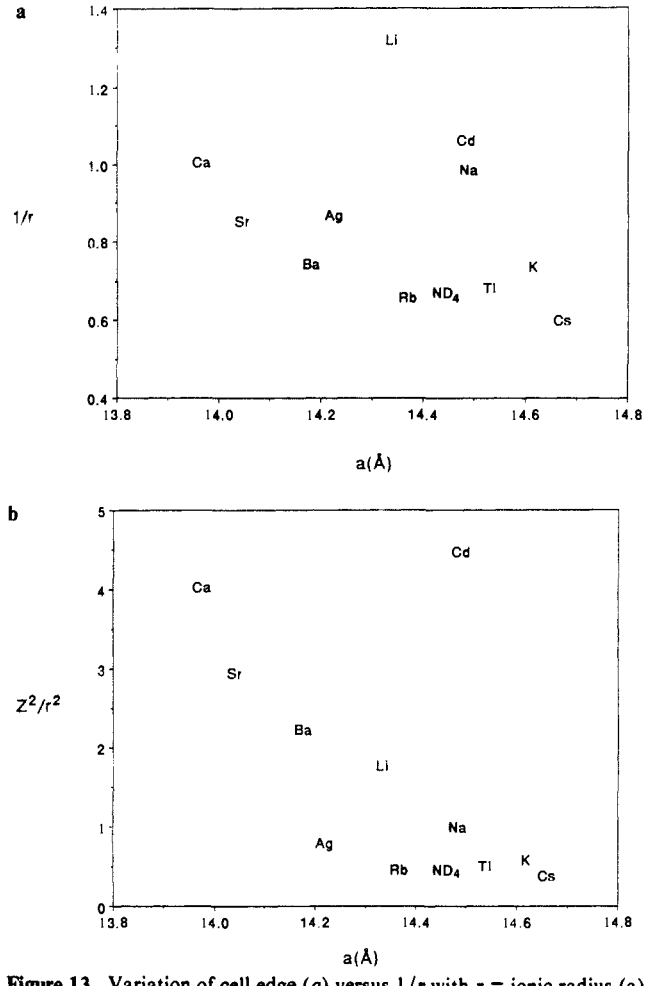

Figure 13. Variation of cell edge (a) versus $1/r$ with r = ionic radius (a) and versus Z^2/r^2 with Z = ionic charge (b).

Indeed, it is clear (Figures 13a and 13b) that the degree of the observed distortions in zeolite RHO is related to the ionic size and charge of the ion-exchanged cation. The lattice parameter and Δ appear to be effective indications of the strength of interaction of the RHO framework (negatively charged) and the charge compensating cations. The limit of the distortion can therefore be tested experimentally by using cations with larger charge/radius ratios, such as Mg^{2+}, Be^{2+}, or Al^{3+}. In fact, Be-RHO is distorted from cubic to lower symmetry and can be indexed as tetragonal with $a = b = 13.192$ (2) Å, $c = 9.268$ (1) Å. The ratio of a:b is 1.423, so that a and b are approximately $\sqrt{2} \times c$. The details of this structure as well as those of the above and other multivalent cation substituted RHO zeolites are presently being determined in order to test the DLS results.

Conclusions

We have synthesized and determined unit cell constants of less than 14.5 Å for ten different ions (Cd, Na, Tl, ND_4, Rb, Li, Ag, Ba, Sr, and Ca). These are the smallest reported unit cells of RHO. The cell dimensions refined for these samples of Ca^{2+}-exchanged zeolite RHO are the smallest observed to date. This observation underscores the flexibility and the stability of the RHO framework whose distortion is a direct measure of the strength of interaction of the charge-compensating cations. Thus, the framework of zeolite RHO can be manipulated from about 15.1 to 13.965 Å by suitable ion exchange and calcination procedures. At the atomic level, this is accomplished via the unusual utilization of tetrahedrally coordinated Ca^{2+}. This ability to modify the dimensions of the internal void volume of a specific molecular sieve is a particularly valuable asset in defining size/shape dependent sorption behavior for the tailoring of catalysts for reactant, product, or transition-state specificity.

Acknowledgment. The authors acknowledge E. T. Jones, Jr., H. Skorny, J. Arena, R. W. Shiffer, J. S. Frieda, C. E. Perry, and R. W. Nickle (deceased) for technical assistance, R. L. Harlow for helpful discussions, as well as support by the Division of Materials Sciences, U.S. Department of Energy under Contract DE-AC02-76CH0016 (DEC) and the Office of Naval Research (GDS).

Supplementary Material Available: Sequences of X-ray diffraction patterns for Ca,Cs-RHO, Ca-RHO, Sr-RHO, and Ba-RHO (Figures 14A-B, 15A-B, 16A-B, and 17A-B, respectively) and tables of refined unit cell dimensions for Ca,Cs-RHO, Ca,NH_4-RHO, Ca-RHO, Sr-RHO, Ba-RHO, and Cd-RHO (Tables VI-A, VI-B, VI-C, VI-D, and VI-E, respectively) (15 pages). Ordering information is given on any current masthead page.

(32) Fischer, R. X.; Baur, W. H.; Shannon, R. D.; Staley, R. H.; Abrams, L.; Vega, A. J.; Jorgensen, J. D. *Acta Cryst.* **1988**, *B44*, 321–334.
(33) Baur, W. H.; Fischer, R. X.; Shannon, R. D.; Staley, R. H.; Vega, A. J.; Abrams, L.; Corbin, D. R.; Jorgensen, J. D. *Z. Kristallogr.* **1987**, *179*, 281–304.